52. Sankaran, H., Sharma, S. M. and Sikka, S. K., *J. Phys., Condens. Matter*, 1992, **4**, L61–L66.
53. McMahan, A. K. and LeSar, R., *Phys. Rev. Lett.*, 1985, **54**, 1929–1932; Mailhiot, C., Yang, L. H. and McMahan, A. K., (preprint) to be published.
54. Reichlin, R., Schiferl, D., Martin, S., Vanderborgh, C. and Mills, R. L., *Phys. Rev. Lett.*, 1985, **55**, 1464–1467; Bell, P. M., Mao, H. K. and Hemley, R. J., *Physica*, 1986, **B139&140**, 16–20.
55. Radousky, H. B., Nellis, W. J., Ross, M., Hamilton, D. O. and Mitchell, *Phys. Rev. Lett.*, 1986, **57**, 2419–2422.
56. Ruoff, A. L., in *Recent Trends in High Pressure Research*, Proceedings of XIII AIRAPT Int. Conf. on High Pressure Science and Technology (ed. Singh, A. K.), Oxford & IBH, New Delhi, 1992, pp. 769–778.
57. Sikka, S. K., Godwal, B. K. and Rao, R. S., *High Pressure Res.*, 1992, **10**, 707–709.
58. Ruoff, A. L. and Luo, H., in *Recent Trends in High Pressure Research*, Proceedings of XIII AIRAPT Int. Conf. on High Pressure Science and Technology (ed. Singh, A. K.), Oxford & IBH, New Delhi, 1992, pp. 779–781.
59. Biswas, R., Martin, R. M., Needs, R. J. and Nielsen, O. H., *Phys. Rev.*, 1984, **B30**, 3210–3213.

11 December 1992; accepted 18 January 1993

RESEARCH ARTICLES

A thermodynamic protocol for explaining subcriticality and other subtle features in self-deflagrating solids

K. Kishore, K. Sridhara and S. Sankaralingam

Department of Inorganic and Physical Chemistry, Indian Institute of Science, Bangalore 560 012, India

A novel universal approach to understand the self-deflagration in solids has been attempted by using basic thermodynamic equation of partial differentiation, where burning rate depends on the initial temperature and pressure of the system. Self-deflagrating solids are rare and are reported only in few compounds like ammonium perchlorate (AP), polystyrene peroxide and tetrazole. This approach has led us to understand the unique characteristics of AP, viz. the existence of low pressure deflagration limit (LPL, 20 atm), hitherto not understood sufficiently. This analysis infers that the overall surface activation energy comprises of two components governed by the condensed phase and gas phase processes. The most attractive feature of the model is the identification of a new subcritical regime I′ below LPL where AP does not burn. The model is aptly supported by the thermochemical computations and temperature-profile analyses of the combustion train. The thermodynamic model is further corroborated from the kinetic analysis of the high pressure (1–30 atm) DTA thermograms which affords distinct empirical decomposition rate laws in regimes I′ and I (20–60 atm). Using Fourier–Kirchoff one dimensional heat transfer differential equation, the phase transition thickness and the melt-layer thickness have been computed which conform to the experimental data.

A mixture of oxidizer and fuel is well known to undergo a self-sustained combustion, i.e. once ignited the material will burn at a certain rate till it is over. Sometimes a single molecule, having fuel and oxidizer elements in them, can also burn on its own—a phenomenon which is known as self-deflagration or auto-combustion. Such compounds are potentially attractive as special fuels. There are only a limited number of self-deflagrating compounds that are known and most of them are liquids like hydrazine, propyl-nitrate, nitromethane, etc. Excluding explosives which do not combust in a controlled fashion, self-deflagrating solids are still scarce. Polystyrene peroxide (PSP), a gummy solid, belongs to a unique class of polymers that exhibit autopyrolysis and auto-combustion[1]. The organic solid tetrazole[2] also supports its own deflagration. The extensively studied molecule, ammonium perchlorate (AP), is yet another example of a self-deflagrating solid[3]. However, its decomposition mechanism is debated[4] and several combustion features are not clearly understood. One of the most striking characteristics of AP combustion is the existence of a critical low pressure deflagration limit (LPL, 20 atm) below which it does not burn. The available literature neither provides any insight into the phenomenon nor the combustion characteristics in the subcritical regime. We have developed a simple *de novo* thermodynamic model not only to understand the existence of LPL and

the features of a new subcritical deflagration regime, below 20 atm which we have christened as a new regime I′, but also to explain several other subtle countenances of AP-fuel systems[5]. This model is aptly supported from independent thermochemical computations and experimentally obtained temperature profiles. Discussing briefly the thermodynamic model we present here a novel kinetic approach which clearly supports the existence of the subcritical deflagration regime I′. Other subtle features like phase transition thickness and melt layer thickness, derived from one-dimensional heat transfer equation and thermochemical approach, are also presented.

Experimental

About 0.02 kg of twice recrystallized AP of particle size 200–250 μm was pelletized in a hydraulic press at 1500 kg cm^{-2} to a density of 1,892 ± 0.003 g cm^{-3}. Cylindrical strands of 4 to 5 mm dia and 30 mm length were cut from the pellet and smoothened using fine emery paper. For determining the burning rate ($\dot{r}$), a high pressure bomb was assembled which had a provision to maintain the sample at a desired pressure (P) and initial temperature (T_0). The bomb was pressurized by Ar or N_2 gas and $\dot{r}$ determined at various P and T_0. It had a provision to record $\dot{r}$ and time–temperature profile using a chromel-alumel microthermocouple fed to a storage oscilloscope. This profile was also used to determine the surface temperature (T_s), the details of the measurements are given elsewhere[5].

High pressure decomposition studies were carried out in a specially designed bomb having facility for differential thermal analysis. The sample temperature (T) and the differential temperature (ΔT) with respect to alumina were recorded on a strip chart recorder. Sample weight of 10 mg and heating rate of 20° C min^{-1} were used in all the runs. Under these conditions no ignition but only decomposition of the sample occurs. Pressure was generated using dry nitrogen gas. Temperature measurement involved an error of ±2° C.

For experimentally determining the critical T_0 at which AP sustains combustion at 1 atm, the following apparatus was used. A bottom-closed cylindrical furnace of 9 cm diameter having an asbestos platform to hold the sample strand at the centre was used. The temperature of the furnace was precisely monitored to a ±1° C accuracy. The AP strand was kept over the platform and allowed to equilibrate with the temperature of the furnace for about half an hour. A mirror fitted at 45° angle atop the opening of the furnace facilitated the visual observation of AP burning. AP was ignited and viewed through the mirror. The experiment was repeated at intervals of 2–3 K starting from 503 K. At about 520 K, the sample sustained combustion and above this temperature the ignition was very smooth and AP burnt homogeneously. The temperature 520 K could therefore be taken as a critical temperature below which AP will not burn at atmospheric pressure. This compares well with the theoretically predicted temperature (523 K).

Results and discussion

The linear regression rate ($\dot{r}$) of the deflagration train of a compressed strand of powder AP strongly depends upon the pressure (P) and initial temperature (T_0). The strand density has negligible effect on LPL. The partial differential equation for the dependence at $\dot{r}$ on P and T_0 can be written as:

$$\mathrm{d}\ln\dot{r} = \left[\frac{\partial \ln \dot{r}}{\partial T_0}\right]_P \mathrm{d}T_0 + \left[\frac{\partial \ln \dot{r}}{\partial P}\right]_{T_0} \mathrm{d}P, \tag{1}$$

$\dot{r}$ depends on surface temperature (T_s), P and T_0 by the equations $\dot{r} = A \exp[-E_s/RT_s)$, $\dot{r} = aP^n$ and $\sigma_p = (\partial \ln \dot{r}/\partial T_0)_p$ respectively, where E_s is the surface activation energy, a is a constant, n the pressure exponent, R the gas constant and σ_p the temperature sensitivity of burning rate. By substituting these quantities in eqn. (1) we get

$$E_s = \left[\frac{\sigma_p R T_s^2}{(\mathrm{d}T_s/\mathrm{d}T_0)_p}\right] + \left[\frac{(n/P) R T_s^2}{(\mathrm{d}T_s/\mathrm{d}P)_{T_0}}\right]. \tag{2}$$

Thus, the overall E_s appears to comprise of two terms ($E_s = E_{s,c} + E_{s,g}$), the surface activation energy ($E_{s,c}$) in the condensed phase just below the burning surface and the gas phase activation energy ($E_{s,g}$) just above the surface. The magnitudes of $E_{s,c}$ and $E_{s,g}$ are primarily determined by $(\mathrm{d}T_s/\mathrm{d}T_0)_p$ and $(\mathrm{d}T_s/\mathrm{d}P)_{T_0}$ respectively depending upon the temperature distribution and chemical composition in the condensed phase. The quantities σ_p, T_s, $(\mathrm{d}T_s/\mathrm{d}T_0)_p$, n and $(\mathrm{d}T_s/\mathrm{d}P)_{T_0}$ were experimentally determined for AP from $\dot{r}$ data and temperature profile analyses. The $E_{s,c}$ and $E_{s,g}$, thus computed from eqn. (2), are given in Table 1.

Different $E_{s,c}$ values in regimes I (20–60 atms) and I′ (below 20 atm) for AP suggest that the combustion mechanism of regime I′ is different from that in I and justifies the identification of regime I′ as new. Analysis of quenched burning AP surface reveals porous structure having cluster of dents with liquid sticking to the wall of the cavity[5]; the liquid analysed is $HClO_4$. No acid is formed in regime I. We have found that AP recrystallized from $HClO_4$ (also from HNO_3, HCl ref.

Table 1. Activation energies and enthalpic data

Systems	Pressure regime (atm)	$E_{s,c}$ (kcal/mole)	$E_{s,g}$ (kcal/mole)
AP	I′	5.3±0.2	10.5±1.5
AP	I	35±1.0	25.0±1.0

ΔH (AP, computed thermochemically) : $\Delta H=274$; $\Delta H_1=77$; $\Delta H_2=197$
ΔH (AP, experimental $\dot{q}$ vs T profile) : $\Delta H=270$; $\Delta H_1=77$; $\Delta H_2=193$

ΔH in cals/g.

6) catalyse the decomposition of AP. Thus, the acid formation explains the low $E_{s,c}$ in regime I′. This low activation energy is consistent with that measured from electrical conductivity studies (5–6 kcal mole^{-1}) corresponding to the speculated[7] charged species such as $NH_4^+ \cdot HClO_4$ and $H_3^+O \cdot HClO_4$. Our identification of $HClO_4$ confirms the formation of the above species.

Thermochemical approach was adopted to understand the LPL and to find the surface heat release in regimes I′ and I. The total heat (ΔH) required to raise the temperature of AP from T_0 to T_f is given by

$$\Delta H=\Delta H_1+\Delta H_2=[C_{po}(T_{tr}-T_0)+\Delta H_{tr}+C_{pc}(T_m-T_{tr}) + \Delta H_m+C_{pm}(T_s-T_m)]+[C_{pg}(T_f-T_s)], \quad (3)$$

where T_{tr}, T_m and T_f are the phase transition, melting and flame temperatures; ΔH_{tr} and ΔH_m are the heats of phase transition and melting; C_{po}, C_{pc}, C_{pm} and C_{pg} are the heat capacities of orthorhombic, cubic, melt and gaseous products respectively. Substituting the appropriate physical constants[5] at LPL, under adiabatic conditions, the total heat ($\Delta H=432$ cal g^{-1}) must be self-generated by the condensed ($\Delta H_1=263$ cal g^{-1}) and gas phase ($\Delta H_2=169$ cal g^{-1}) just sufficient to support combustion in their respective regimes. ΔH_1 is in fact equivalent to exothermic heat of decomposition of AP ($\Delta H_d=265$ cal g^{-1}) the only source of heat in the condensed phase, it implies that ΔH_2 is the heat generated to maintain combustion in the gas phase.

At 1 atms (regime I′), $\Delta H=274$ cal g^{-1} is composed of $\Delta H_1=77$ cal g^{-1} the heat required to raise the temperature from critical T_0 (at 1 atm AP does not burn below 520 K) to T_s, and $\Delta H_2=197$ cal g^{-1}. Since the variation of T_f with pressure is negligible[8,9], it may be assumed that $\Delta H_{2(LPL)}$ remains independent of the pressure. The excess gas phase heat release ($\Delta H_{2\ (1\ atm)} - \Delta H_{2(LPL)}=28$ cal g^{-1}) comes from AP decomposition making thus 105 cal g^{-1} as the total heat generated in the condensed phase. This subdued heat release which falls short of the LPL critical enthalpy (265 cal g^{-1}) and prevents sustenance of combustion below LPL is due to the AP sublimation which occurs to an extent of 21%. The fraction of AP subliming decreases with increase in pressure till LPL where it vanishes.

Above LPL (regime I), the flame moves closer to the surface resulting in excess heat transfer ($\Delta H_1-\Delta H_d$) to the surface which is used in AP melting. This heat transfer increases with pressure and follows the trend of the melt layer thickness in regime I.

To substantiate the above thermochemical analysis, temperature profiles were transformed into heat release rate ($\dot{q}$) vs temperature (T) curves by multiplying the slope at the mean temperature by the heat capacity (C_p)[1]. A typical computer generated $\dot{q}$ vs T curve (Figure 1) shows a sharp dip (arrow marked) corresponding to the burning surface and is concordant with the independently measured T_s. Such curves are akin to DSC thermograms[1]; the multiple peaks in the condensed and gas phases (Figure 1) suggest a complex combustion process. The enthalpies ΔH, ΔH_1 and ΔH_2 (Table 1) obtained from these $\dot{q}$ vs T curve by area measurements match with those obtained from thermochemical calculations using eqn. (3).

The critical condensed phase enthalpy (ΔH_1) for AP burning at 1 atm is 105 cal g^{-1} but it will burn only at its critical T_0 which is 520 K. If AP were made to burn at 1 atm but at 300 K, the critical enthalpy (ΔH_1) would be 179 cal g^{-1}. In order to verify this critical enthalpy, the stoichiometric mixture of AP + organic fuel system which can burn at room temperature (say 300 K) and 1 atm was considered. It is imperative that the enthalpy of this AP + organic fuel, which falls short of the critical value 179 cal g^{-1}, will not sustain combustion. AP + aliphatic dicarboxylic acid fuel system was investigated and the temperature–time profile of the combustion train was experimentally obtained. The measured temperature–time profiles were converted, by computer, into $\dot{q}$ vs temperature curves. The heat capacity of the mixture, $C_{p,\ mixt}$, used for the $\dot{q}$ estimation requires the knowledge of the heat capacity of the dicarboxylic acids as well as AP at different temperatures. The heat capacity of AP in the orthorhombic and cubic regions was taken from

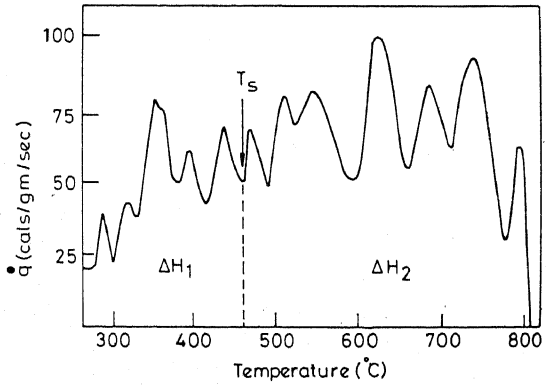

Figure 1. $\dot{q}$ vs T profile of AP at $T_0=520°$C and 1 atm.

elsewhere[5]. The C_p data of the acid fuels are not available in the literature, they were experimentally determined using DSC. The following equation fits the C_p–temperature data,

$$C_p = \alpha + \beta T. \quad (4)$$

The best fit constants α and β for the acids are given in Table 2. At any given temperature, the C_p (cal g^{-1} deg^{-1}) of the AP/fuel mixture was calculated from the following equation

$$C_{p,\,mixt} = \omega_0 C_{po} + \omega_f C_{pf}, \quad (5)$$

where ω_0 and ω_f are the weight fractions and C_{po} and C_{pf} are the heat capacities of the oxidizer and fuel respectively. The $\dot{q}$ vs temperature curves for different fuel systems are shown in Figures 2 and 3. The arrow mark indicates the burning surface which deciphers the condensed phase reactions occurring below it and the gas phase reactions above it. The $\dot{q}$ vs T profiles were used to compute the condensed phase enthalpies (ΔH_1) by measuring area under the curve and multiplying it by the time interval elapsed. The gas phase enthalpies (ΔH_2) could not be obtained from the temperature profile data due to the melting of the microthermocouple. The ΔH_1 values are given in Table 2, as the molecular weight increases, the ΔH_1 with respect to AP also increases. Since critical ΔH_1 for AP to sustain combustion, at 1 atm and 300 K, is 179 cal g^{-1}, this suggests that AP/fuel mixture, below succinic acid whose ΔH_1 is 186 cal g^{-1}, will not sustain combustion. Indeed AP/malonic acid does not burn at all, the extrapolated ΔH_1 obtained from Table 2 for this system is 50 cal g^{-1} which is far too low from the critical value for sustaining combustion. This result gives credence to our enthalpic computations.

Similar temperature-profile analysis in PSP autocombustion[1,10] suggests the existence of maximum temperature region between the surface and the flame because the energy required to raise the temperature of the solid from T_0 to T_s is much smaller compared to

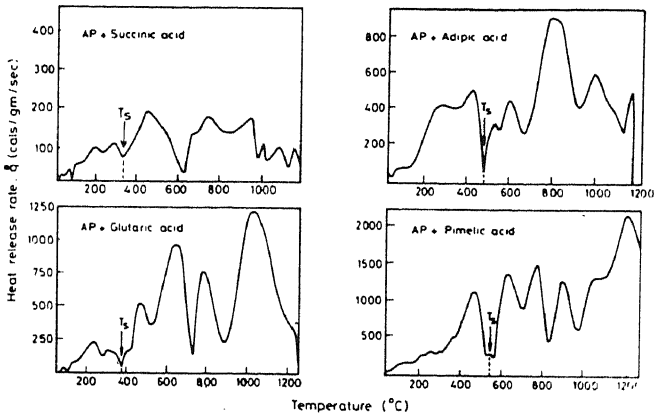

Figure 2. $\dot{q}$ vs T profiles of AP + dicarboxylic acid mixtures burning at 1 atm.

the heat of degradation of PSP and hence aldehyde vapours emanating from the surface get appreciably heated up by the excess energy of pyrolysis. This sets up a hot vapour zone between the surface and the flame. It is this excess enthalpy that is responsible for a very high rate of auto-pyrolysis and auto-combustion similar to that observed in propellants.

Only few studies have been carried out in the past on AP decomposition at high pressures[11–13], the analysis of these studies shows that (i) phase transition remains unaltered, (ii) the low temperature exotherm does not show any appreciable change, and (iii) as the pressure is increased high temperature exothermic peak becomes sharper and the decomposition temperature is lowered suggesting that AP decomposition gets accelerated. However, no explanation is available as to how the pressure affects the AP decomposition. In the present investigation an attempt is made to analyse the effect of pressure on AP decomposition. There are two major views relating to the mechanism of decomposition of AP namely (i) electron transfer and (ii) proton transfer. The consensus seems to have veered around the latter approach, particularly so under combustion conditions. In the present investigation the proton transfer mechanism is assumed to hold good particularly under

Table 2. Heat capacity constants and condensed phase enthalpies of AP-dicarboxylic acid system

Acid system	α	$\beta \times 10^3$	Wt.% of AP/acid in the mixture	Condensed phase enthalpy (ΔH_1) in cal/g. ΔH_1 (mix.)	ΔH_1 (AP)
Succinic acid	0.226	1.32	73.6/26.4	137	186
Glutaric acid	0.264	0.65	78.1/21.9	240	308
Adipic acid	0.267	1.04	80.7/19.3	362	448
Pimelic acid	0.214	1.72	82.5/17.5	377	457
Suberic acid	0.234	1.56	83.7/16.3	387	162
Azelaic acid	0.300	1.18	84.6/15.4	404	477
Sebacic acid	0.217	1.95	85.3/14.7	443	520

Wt.% of AP/acid in the mixture corresponds to the stoichiometric composition.

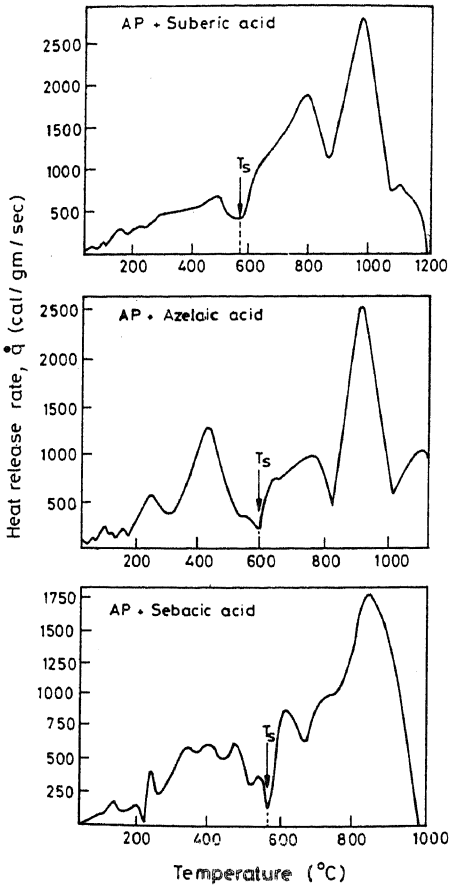

Figure 3. $\dot{q}$ vs T profiles of AP + dicarboxylic acid mixtures burning at 1 atm.

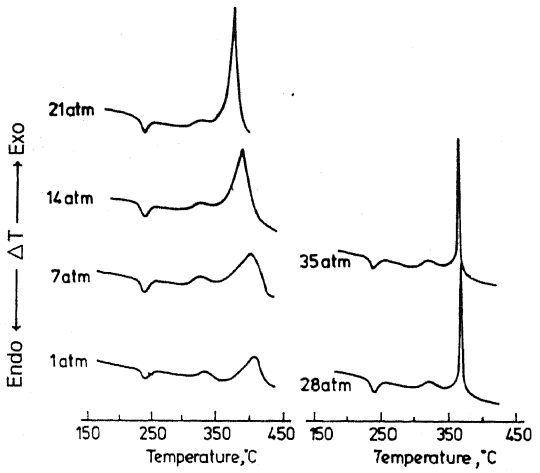

Figure 4. High pressure DTA trans of AP.

closed conditions,

$$NH_4ClO_4 \underset{k_2}{\overset{k_1}{\rightleftharpoons}} NH_3 + HClO_4 - 58 \text{ kcal} \qquad (6)$$

$$2N_2 + \xrightarrow{k_3} \text{Decomposition} \quad \Delta H. \qquad (7)$$

The thermograms obtained as a function of pressure are given in Figure 4. The peak temperatures of the exotherms are given in Table 3. The data of Waesche and Wenograd[12] were analysed to obtain peak temperatures and they are also included in Table 3 for comparison. The disagreement at the absolute values is attributed to the particle size, purity[14,15] of the sample and equipment employed. However, the trends are the same as can be seen from the reduced plot (Figure 5) of T_p/T_p^* vs P (T_p^* is the peak temperature, T_p, at one atm). In other words, there is agreement in that the decomposition is sensitized as the pressure is increased. Such a conclusion is also consistent with other observations[11,13,16].

The molar equilibrium constant, K_c, with reference to eqn. (6) can be written as

$$K_c = \frac{\alpha^2}{(1-\alpha)(1+\alpha+n)}, \qquad (8)$$

Table 3. Effect of pressure on AP decomposition temperature

Sample weight = 10 mg
Atmosphere = nitrogen
Heating rate = 20° C/min.

Pressure/atm.	Peak temperature (K)
1	679 (725*)
4	719*
7	673
14	661
17	709*
21	648
28	641
30	690*
35	637

*Waesche and Wenograd data.

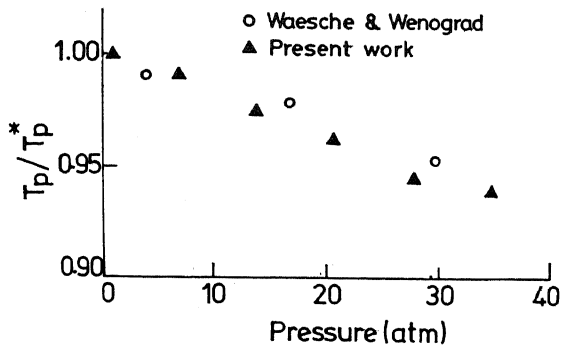

Figure 5. Plot of T_p/T_{p^*} against pressure.

where α is the fraction of AP decomposed and n is the number of moles of the inert gas N_2. The partial pressure equilibrium constant, K_p, is related to the molar equilibrium constant K_c ($K_p = K_c P^{\Delta n'}$); $\Delta n'$ is the difference between the number of moles of the product and the reactant species. In the present case $\Delta n' = 1$ and

therefore

$$K_p = \frac{\alpha^2 P}{(1-\alpha)(1+\alpha+n)}. \quad (9)$$

It is assumed that N_2 obeys ideal gas behaviour and $n \gg (1+\alpha)$. Since decomposition is carried out at a constant volume ($n = C_1 P$, where $C_1 = V/RT$), eqn. (9) reduces to

$$K_p = \frac{\alpha^2}{(1-\alpha)C_1}. \quad (10)$$

In the above equation, K_p is independent of P and leads us to conclude that eqn. (6), corresponding to the dissociation equilibrium, is insensitive to the inert gas pressure. This implies that N_2 pressure affects only the reaction shown in eqn. (7).

Decomposition can be accelerated by N_2 either by activating $HClO_4$ decomposition alone (case 1) or by accelerating the reaction between $HClO_4$ and NH_3 (case 2).

Case 1

$$HClO_4 + xN_2 \xrightarrow{k_4} HClO_4^* + xN_2 \quad (11)$$

$$HClO_4^* \xrightarrow{k_5} \text{decomposition products} \quad (12)$$

The rate of product formation (dB/dt) is then

$$(dB/dt) = K_5 (HClO_4)^* = K_4 (HClO_4)(N_2)^x. \quad (13)$$

Case 2

$$NH_3 + HClO_4 + xN_2 \xrightarrow{k_6} NH_3^* + HClO_4^* + xN_2 \quad (14)$$

$$NH_3^* + HClO_4^* \xrightarrow{k_7} \text{decomposition products} \quad (15)$$

Here, the analogue of eqn. (13) is

$$(dB/dt) = K_7 (NH_3^*)(HClO_4^*) = k_6 (NH_3)(HClO_4)(N_2)^x. \quad (16)$$

In either case [eqns. (11) or (14)] the rate of product formation is directly related to the N_2 pressure.

In differential scanning calorimetric (DSC) experiments, the ordinate deflection corresponds to the rate of reaction. The rate of product formation could therefore be taken as the rate of heat production (dH/dt), from eqns. (13) and (16) we can write

$$(dH/dt) = k_4 (HClO_4)(N_2)^x = k_6 (AP)(N_2)^x. \quad (17)$$

Eqn. (17) leads to the following general form

$$(dH/dt) = C_2 A \exp(-E/RT)(N_2)^x, \quad (18)$$

where the constant C_2 takes into account all the concentration terms. The terms A, E and R are the frequency factor, activation energy and gas constant respectively. Eqn. (18) describes the kinetics of AP decomposition; the DSC thermogram, which essentially gives the rate of heat release ($-dH/dt$) as a function of temperature (T), can be represented by the following equation for AP decomposition.

$$\frac{d(dH/dt)}{dT} = \frac{d[C_2 A \exp(E/RT) P^x]}{dT}. \quad (19)$$

At the peak temperature, T_m, where (dH/dt) is maximum, the (d/dT) (dH/dt) is zero, as a result eqn. (19) takes the following form

$$\ln P = \frac{E}{Rx}\frac{1}{T_m} + C. \quad (20)$$

The peak temperature (T_m) as a function of pressure can be obtained both from high pressure DTA and high pressure DSC. The plot of ln P vs $1/T_m$ is shown in Figure 6. It provides two slopes and the values are consistent with the data of Waesche and Wenograd too. Interestingly the different slopes once again reflect the two distinct regimes I′ and I. This kinetically derived result further supports the results derived from thermodynamic model discussed earlier. From the slope, the exponent x was obtained which gave the following empirical decomposition rate law.

$$d \simeq a' p^{0.3} \text{ (regime I′)} \quad (21)$$

$$d \simeq a' p^{2.0} \text{ (regime I)}. \quad (22)$$

It is evident that the pressure sensitivity of the decomposition rate is considerably lower in regime I′

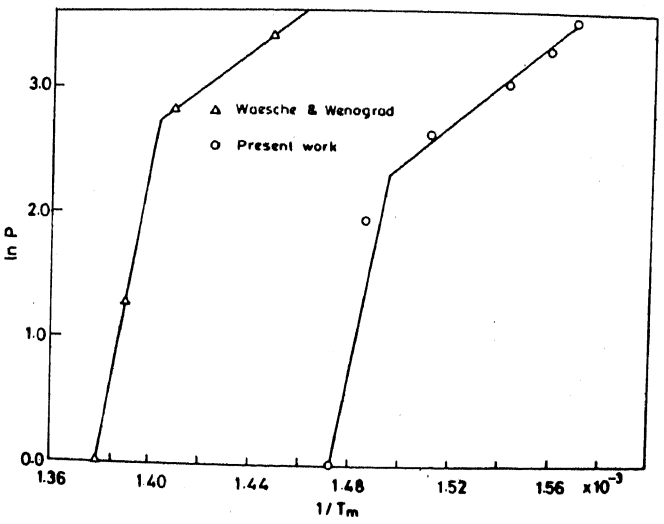

Figure 6. Plot of ln$P$ vs $1/T_m$.

which may be attributed to the substantial sublimation of AP in regime I′ as discussed earlier. The above empirical decomposition laws can be compared with the empirical burning rate law[5].

$$\dot{r} \simeq a P^{0.9} \text{ (regime I')} \tag{23}$$

$$\dot{r} \simeq a P^{0.8} \text{ (regime I)}. \tag{24}$$

In regime I, where no sublimation is observed, thermal degradation significantly influences the burning rate. About 2.5 units change in decomposition rate brings about one unit change in $\dot{r}$. Interestingly this result is concordant with our earlier observation on the role of condensed phase reactions in AP+polymeric fuel combustion where three-unit change in decomposition brings about one-unit change in the burning rate[3].

AP deflagration is pictorically represented in Figure 7. Since AP strand is side insulated to achieve linear regression, the surface could be considered as a heat source through which heat is transferred deep into the solid vertically along the Y-axis. Under steady state combustion, the heat is transferred from the flame to the surface which in turn generates a temperature gradient below the surface. Thus, the surface can be taken as a plane of heat source of uniform intensity, propagating in one dimension with a uniform velocity $\dot{r}$. This can be represented mathematically by the Fourier–Kirchoff differential equation for one dimensional heat transfer along the Y-axis.

$$K(\partial^2 T/\partial Y^2)_t = \rho C_p (\partial T/\partial t)_Y \tag{25}$$

Heat gain in certain volume per sec. — Rise in temperature

where K is thermal conductivity, C_p the specific heat, ρ the density of the condensed-phase below the surface, T the temperature, t the time and Y the space coordinate.

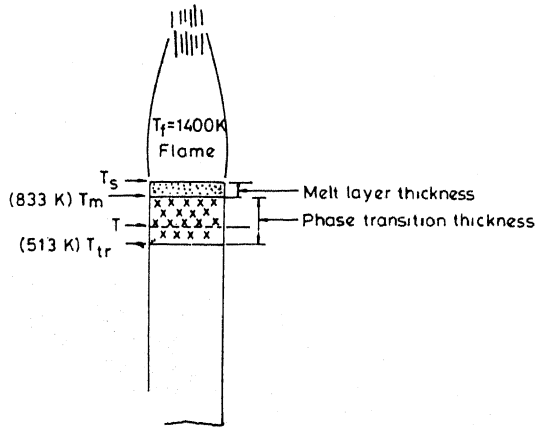

natic representation of AP combustion.

It is convenient to consider the distance with respect to the surface and therefore one can carry out the following coordinate transformation in the moving frame of reference.

$$X = Y - \dot{r}t, \tag{26}$$

where X represents the distance from the surface in Y coordinate. The differential eqn. (25) can now be rewritten as

$$K(\partial^2 T/\partial X^2)_t = \rho C_p [(\partial T/\partial t)_X - \dot{r}(\partial T/\partial X)_t]. \tag{27}$$

At steady state, $(\partial T/\partial t)_X = 0$, therefore, eqn. (27) reduces to

$$K(\partial^2 T/\partial X^2)_t = -\rho C_p \dot{r}(\partial T/\partial X)_t. \tag{28}$$

The general solution of the above differential eqn. (28) is given below

$$T = C_1 + C_2 \exp(-\dot{r}X/\alpha), \tag{29}$$

where α is the thermal diffusivity, C_1 and C_2 are constants which could be evaluated by using proper boundary conditions: When X is 0, T is equal to the surface temperature (T_s) and when X goes to infinity T is equal to T_0. The eqn. (29) then takes the following form

$$X = (\alpha/\dot{r}) \ln (T_s - T_0/T - T_0). \tag{30}$$

By substituting the critical burning rate at 20 atm ($\dot{r}$=0.33 cm s^{-1}) and the corresponding T_s=833 K, melting temperature (T_m)=833 K, α (cubic AP) 1.1 × 10^{-3} and T_0=300 K, the phase transition thickness (X_{tr}) can be calculated from eqn. (30). The (X_{tr}) was calculated at various $\dot{r}$ values (Figure 8). The phase transition thickness has been experimentally measured

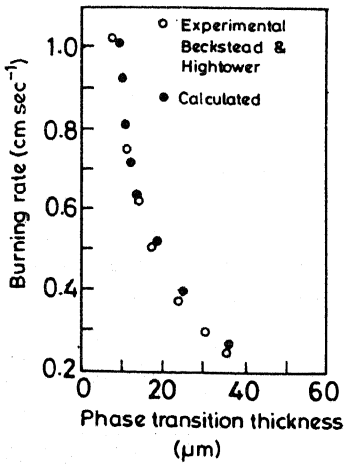

Figure 8. Variation of burning rate on the phase transition thickness.

by Beckstead and Hightower[17]. The dependence of X_{tr} on $\dot{r}$ is also shown in Figure 8 which is agreeable with the experimental values[17].

From scanning electron microscope (SEM) studies the presence of the melt on the surface of burning AP has been shown by Hightower and coworkers[17,18]. They concluded that the melt layer thickness (m) decreases as the pressure is increased but gave no quantitative information. Guirao and Williams[8] gave a quantitative picture of the dependence of m on pressure and showed that m increases with pressure (Figure 9).

Boggs and Kraeutle[19] analysed the quenched AP samples in the pressure range 20–60 atm by using SEM. They observed that the surface was covered with froth which was due to the presence of liquid layer. Between 20 and 40 atm the froth was shown approximately to be 3 to 5 μm thick and therefore it may be concluded that the melt layer on the AP crystal surface may be of the order of 3–5 μm. Using eqn. (30), m was calculated from the following equation, employing $\dot{r}$ and T_s data[8,9] and α (melt) $= 1.77 \times 10^{-3}$; the results are shown in Figure 9.

$$m = \frac{(1.77)\ 10^{-3}}{\dot{r}} \ln \frac{T_s - 300}{833 - 300}. \qquad (29)$$

We make the following observations: (i) Below a critical m corresponding to 20 atm combustion does not sustain, and (ii) the variation of m with pressure in regimes above I follows the same trend as reported by Guirao and Williams[8] that it increases first, reaches a maximum and then decreases. This trend is similar to the one proposed by Boggs[20] for the change in $\dot{r}$ as a function of pressure (see inset of Figure 9). Thus, one is tempted to conclude that the burning of AP is greatly influenced by the melt. The values of m obtained in the present calculation are nearer to the experimental values[19] than computed values reported by Guirao and Williams[8].

Boggs and Kraeutle[19] observed a significant melt up to 65 atm but in the pressure range 70–140 atm they observed comparatively less liquid on the surface. The optimum pressure range where melt is observed from our calculations is 20 to 200 atm. The calculated value of m around 200 atm suggests that burning rate should drastically decrease. Levy and Friedman[21] and Glaskova[22] have reported the upper pressure deflagration limit (UPL) around 250 atm. This UPL is very close to the one predicted by calculations of m. Although the later works by Boggs[20] disproved the existence of UPL, it may be noted that UPL may exist when small diameter ($\ll 7$ mm) samples are used. The present calculations suggest that $\dot{r}$ should drastically decrease around 200 atm (Figure 5). It may be noted that AP sustains combustion even at higher pressures beyond 250 atm as shown in Figure 9, but in that region the melt has not been reported and some other mechanism of combustion has been suggested[8].

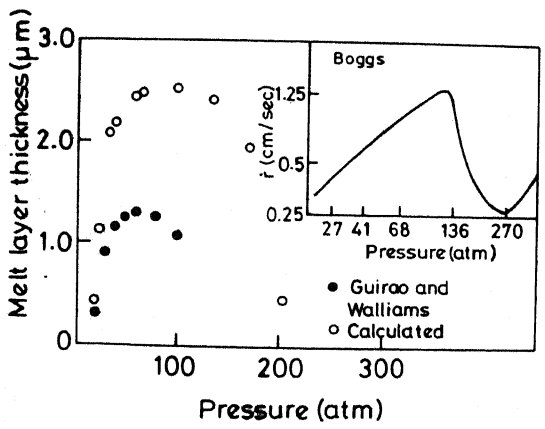

Figure 9. Dependence of $\dot{r}$ and m on pressure.

1. Kishore, K. and Mukundan, T., *Nature*, 1986, **324**, 130–131.
2. Lesnikovich, A. I., Suiridov, V. V., Printsev, G. V., Ivaskhevich, O. A. and Gaponik, P. N., *Nature*, 1986, **323**, 706–707.
3. Kishore, K. and Gayathri, V., in *Fundamentals of Combustion of Solid Propellants* (eds. Kuo, K. K. and Summerfield, M.), American Institute of Aeronautics and Astronautics Inc., New York, 1984, ch. 2, pp. 53–119.
4. Galway, A. K. and Mohamed, M. A., *Nature*, 1984, **311**, 642–645.
5. Kishore, K. and Sridhara, K., *Proc. R. Soc. (London)*, Ser. A., 1992 1993, **440**, 55–76.
6. Pai Vernekar, V. R., Kishore, K. and Gayathri, V., *J. Appl. Chem. Biotechnol.*, 1978, **28**, 660–662.
7. Melik Gaikazov, G. V. and Marshakov, V. N., *Fiz. Goreniya Vzryva*, 1987, **23**, 15–20.
8. Guirao, C. and Williams, F. A., *Am. Inst. Aeron. Astron. J.*, 1971, **9**, 1345–1356.
9. Sohn, H. Y., *Combust. Sci. Technol.*, 1975, **20**, 137–154.
10. Mukundan, T. and Kishore, K., *Curr. Sci.*, 1991, **60**, 355.
11. Stone, R. L., *Anal. Chem.*, 1960, **32**, 1582–1588.
12. Schmidt, W. G., NASA-CR-66757 Report, May 1969, pp. 49.
13. Waesche, R. H. W. and Wenograd, J., Report No. WSC 1–67–8, April 1967 from United Aircraft Research Laboratory, East Haltford, Conn, USA, pp. 1–16.
14. Adams, G. K., Newman, B. H. and Robins, A. B., VIIIth Symposium (Int.) on Combustion, Combustion Institute, Williams and Wilkins, Baltimore, 1962, pp. 693–705.
15. Boggs, T. L., Zurn, D. E. and Netzer, D. W., *Combust. Sci. Technol.*, 1973, **7**, 177–183.
16. Morisaki, S. and Komamiya, K., *Thermochim. Acta*, 1975, **12**, 239–251.
17. Beckstead, M. W. and Hightower, J. D., *Am. Inst. Aeron. Astron. J.*, 1967, **5**, 1785–1790.
18. Beckstead, M. W., Derrr, R. L. and Price, C. F., XIIIth Symposium (Int.) on Combustion, The Combustion Institute, Pittsburg, 1971, pp. 1047–1056.
19. Boggs, T. L. and Kraeutle, K. J., *Combust. Sci. Technol.*, 1969, **1**, 75–93.
20. Boggs, T. L., *Am. Inst. Aeron. Astron. J.*, 1970, **8**, 867–873.
21. Levy, J. B. and Friedman, R., VIIIth Symposium (Int.) on Combustion, Williams and Wilkins, Baltimore, 1962, pp. 663–672.
22. Glaskova, A. P., *Z. Prikl. Mekhan Z⁻. Tekhn Fiz. S. S. R.*, 1963, **5**, 121–125.

Received 26 August 1992; revised accepted 13 January 1993